Invited paper

NEW APPROACHES TO MODELING OF LIGHTNING ELECTROMAGNETIC FIELD

Vesna JAVOR[1], Predrag D. RANČIĆ[2]

Abstract: This paper presents the results of the research on lightning electromagnetic field calculations in time domain in the case of perfectly conducting ground, so as calculations in frequency domain of electromagnetic field radiated by mast antenna above real ground. It should be emphasized that several novel approaches during this research were introduced, including application of one new function for representing lightning return stroke channel-base current and one new model for spectral reflection coefficient for solving problems of the real ground parameters influence.

Keywords: Lightning electromagnetic field, Return stroke current, Antenna, Spectral reflection coefficient.

INTRODUCTION

In the first section of this paper the structure of lightning electromagnetic field (LEMF) is numerically determined directly in time domain using antenna theory approach and thin wire approximation of the lightning channel. Within modified transmission line model with exponential decay, as an engineering return stroke current model, one new suitable function is applied for the approximation of channel-base current. Parameters of this function are chosen so they provide desired characteristics of lightning electromagnetic pulse. The results are in good agreement with the results from literature.

In the second section of the paper the influence of lightning channel height on values of LEMF components is presented. In the near zone of the channel-base, at ground surface points, the influence on electric field components is greater than in the far zone, where this height determines spike in a certain time moment after the onset of lightning electromagnetic pulse (LEMP). Magnetic field for the points at ground surface does not differ a lot for different lightning channel heights for the near zone and for far zone the choice of different channel heights also produces spikes in different time moments as for the electric field. The new simple return stroke channel-base function and determining LEMF in time domain provide very easy analysis of interrupting vertical lightning channel on a certain height from its base, although natural lightning channel conditions necessarily differ from such assumption, especially because of branching and very complicated physical processes during lightning discharge.

The analysis in frequency domain of a vertical mast antenna, which can represent the lightning discharge current channel above the real ground of known electrical parameters, is presented in the third section of the paper. This is necessary in order to perform Fast Fourier Transform (FFT) on the results in frequency domain and then afterwards to obtain results for LEMF components in time domain treating influence of the real ground. This would be much more complicated in time domain directly.

CALCULATING LEMF IN TIME DOMAIN

Theoretical approach

The structure of LEMF is numerically calculated directly in time domain using antenna theory approach and thin wire approximation of the lightning channel. Lightning channel current is modeled using modified transmission line model with exponential decay (MTLE) as one of various proposed engineering lightning channel return stroke current models ([1] and [2]). New suitable function [3] is used within this MTLE model for approximation of lightning return stroke channel-base current [4]. The function and its parameters are analyzed in order to obtain desired LEMP characteristics and to make proper choice of function parameters. The results are in good agreement with the results from [5] and [6]. The function can be easily used for approximating different desired characteristics of lightning return stroke channel-base current such as current peak, rise-time to peak, current steepness and charge transfer. There are also possibilities to adopt function parameters in order to satisfy other demands, such as decreasing-time to half of the peak value, increasing-time, values for the first and higher order derivatives which determine the shape of the function, integral of the function itself or integral of the square of the function, etc.

Lightning current channel is modeled as vertical mast antenna above perfectly conducting ground, having height H and radius r_0, $r_0 << H$, energized by current pulse source at its base (Fig.1). Electric and magnetic field components at the field point $\mathrm{P}(r, \psi, z)$ in time domain, as in [6], [7] and [8], can be expressed in cylindrical coordinates as following:

$$E_z(\vec{R},t) = \frac{1}{4\pi\varepsilon_0}\int_{-H}^{H}\left[\frac{2(z-z')^2 - r^2}{R_k^{\,5}}\int_{\tau=0}^{\tau=t} i\left(z', \tau - \frac{R_k}{\mathrm{c}}\right)\mathrm{d}\tau + \right.$$

[1] University of Nis, Department of Theoretical Electrical Eng., Aleksandra Medvedeva 14, P.O.Box 73, 18000 Nis, Serbia, E-mail: vjavor@elfak.ni.ac.yu

[2] University of Nis, Department of Power Eng., Aleksandra Medvedeva 14, P.O.Box 73, 18000 Nis, Serbia, E-mail: prancic@elfak.ni.ac.yu

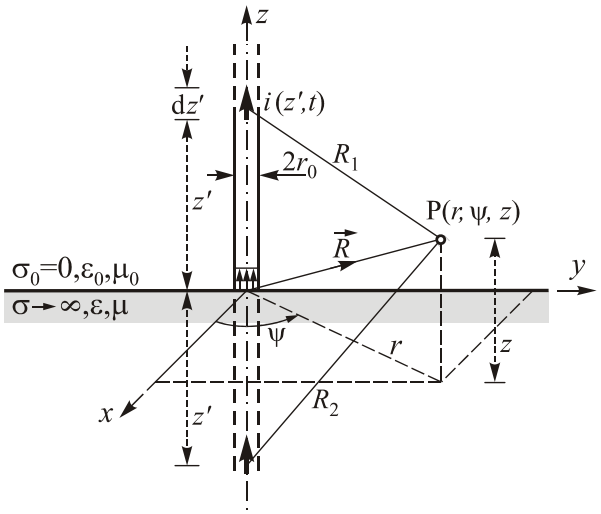

Fig.1 - *Lightning channel current model in the case of perfectly conducting ground.*

$$+\frac{2(z-z')^2-r^2}{\mathrm{c}\,R_k^{\,4}}\,i\left(z',t-\frac{R_k}{\mathrm{c}}\right)-\frac{r^2}{\mathrm{c}^2\,R_k^{\,3}}\,\frac{\partial i\left(z',t-\frac{R_k}{\mathrm{c}}\right)}{\partial t}\Bigg]\mathrm{d}\,z', \quad (1)$$

$$E_r(\vec{R},t)=\frac{1}{4\pi\varepsilon_0}\int_{-H}^{H}\Bigg[\frac{3r(z-z')}{R_k^{\,5}}\int_{\tau=0}^{\tau=t} i\left(z',\tau-\frac{R_k}{\mathrm{c}}\right)\mathrm{d}\tau+$$

$$+\frac{3r(z-z')}{\mathrm{c}\,R_k^{\,4}}\,i\left(z',t-\frac{R_k}{\mathrm{c}}\right)+\frac{r(z-z')}{\mathrm{c}^2\,R_k^{\,3}}\,\frac{\partial i\left(z',t-\frac{R_k}{\mathrm{c}}\right)}{\partial t}\Bigg]\mathrm{d}\,z', \quad (2)$$

and

$$H_\psi(\vec{R},t)=\frac{1}{4\pi}\int_{-H}^{H}\Bigg[\frac{r}{R_k^{\,3}}\,i\left(z',t-\frac{R_k}{\mathrm{c}}\right)+\frac{r}{\mathrm{c}\,R_k^{\,2}}\,\frac{\partial i\left(z',t-\frac{R_k}{\mathrm{c}}\right)}{\partial t}\Bigg]\mathrm{d}\,z', \quad (3)$$

where: E_z – vertical electric field, E_r – radial electric field, H_ψ – azimuthal magnetic field, R_k – the distance from the antenna current element, for k=1, and its image in plane mirror, for k=2, to the field point P, $i(z',t)$ – the lightning channel current, ε_0 – the permittivity of air, $\mathrm{c}=(\varepsilon_0\mu_0)^{-1/2}$ – the speed of light and H – the total height of finite vertical linear antenna on perfectly conducting ground surface.

New return stroke Channel-Base Current (CBC)

Return stroke lightning current models can be categorized in several categories, as e.g. in [1] and [2]. Engineering models specify relation between the current distribution along lightning channel, $i(z',t)$, and current at the channel-base, $i(0,t)$, as following:

$$i(z',t)=u(t-z'/v_f)P(z',t)i(0,t-z'/v), \quad (4)$$

where: $u(t)$ – the Heaviside function, v_f – the return-stroke speed, v – the current-wave propagation speed and $P(z',t)$ – the height- and time-dependent current attenuation factor. There are travelling current source model (TCS), transmission line model (TL), modified TL with linear decay with height (MTLL) or with exponential decay with height (MTLE), modified TL with current distortion (MTLD), etc. For MTLE model attenuation factor $P(z')=\exp(-z'/\lambda)$ is assumed, as only height-dependent, where λ is the adaptive constant and z' the height from the channel base.

For the return stroke lightning channel-base current (CBC) one new function (Fig.2) is used in this paper:

$$I(t)=\frac{i(t)}{I_m}=\begin{cases}\left[\tau\,\mathrm{e}^{(1-\tau)}\right]^a, & 0\le\tau\le 1\\ \left[\tau\,\mathrm{e}^{(1-\tau)}\right]^b, & 1\le\tau<\infty\end{cases} \quad (5)$$

where: a and b – the parameters of the function, $\tau=t/t_m$, t_m – rise-time to peak value and I_m – the maximum current value. The function was earlier used only as the pulse function 1.2/50 in high voltage technique [3], with front rise-time $t_c=1.2\,\mu\mathrm{s}$ and decreasing time to half of the peak value of about $50\,\mu\mathrm{s}$. In that case chosen function parameters values are: a=4, $b=0.0312596735$ and $t_m=1.906398381\,\mu\mathrm{s}$. For the saddle point in the rising part $0\le t\le t_m$ at $\tau_1=t_1/t_m=0.5$, the maximum value of the first derivative is $\mathrm{d}I/\mathrm{d}\tau=1.847$. The value of parameter b is obtained for the function value equal to half of the peak value at $t_k=50.422\,\mu\mathrm{s}$ and then the saddle point in declining part is at $\tau_2=t_2/t_m=6.656$. It should be noticed that the first derivative of the function $i(t)$ is $\mathrm{d}i/\mathrm{d}t=I_m\,\mathrm{d}I/\mathrm{d}t=I_m t_m^{-1}\,\mathrm{d}I/\mathrm{d}\tau$.

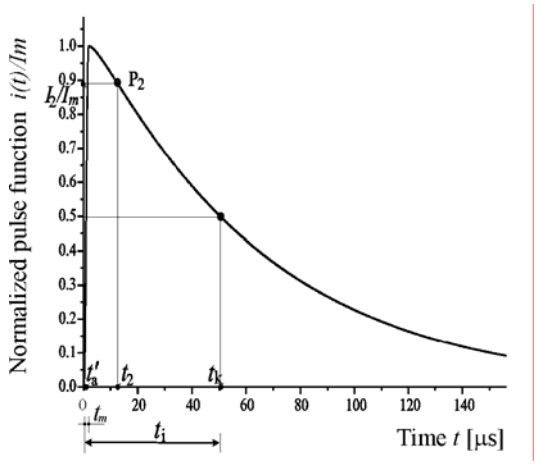

Fig.2 - *Normalized CBC function* $i(t)/I_m$ *versus time* t.

Parameters of the CBC function

Parameters of the CBC function, Eq. (5), can be chosen so that it approximates, for example, commonly used double-exponential function, proposed by Bruce and

Golde in [9] (BG function), or any other pulse function as the return stroke channel-base current. For the BG function at the base $i(t) = I_m(\mathrm{e}^{-\alpha t} - \mathrm{e}^{-\beta t})$, with parameters $\alpha = 3\cdot 10^4\,\mathrm{s}^{-1}$, $\beta = 10^7\,\mathrm{s}^{-1}$, $I_m = 11\,\mathrm{kA}$, $t_m = 0.5826\,\mu\mathrm{s}$, and decreasing time to half of the peak value of approximately $23\,\mu\mathrm{s}$, the following parameters for the proposed CBC function should be chosen $I_m = 11\,\mathrm{kA}$, $t_m = 0.5826\,\mu\mathrm{s}$, a=0.5 and b=0.019. There is no need for the peak correction factor of the maximum current value I_m, as in some other models functions (e.g. [2], [10]).

The first derivative of the CBC function is obtained analytically and is continuous in the peak point. Higher order derivatives are not continuous in that point. Parameter *a* determines current steepness in the rising part of the function ([11]). The dependence of current steepness versus variable τ, for $I_m = 13\,\mathrm{kA}$ and $t_m = 0.5\,\mu\mathrm{s}$ and different *a*, is presented in Figs.3-6.

For the desired current steepness $\mathrm{d}i/\mathrm{d}t$ one can choose for the rising part of the function to have convex shape without saddle point (Fig.3) or convex to concave shape and saddle point in the rising part (Figs.4-6). For convex shape in the rising part of the function the value of parameter *a* is $0 < a < 1$. The BG function also has convex shape in the rising part. For having saddle point in the rising part, as in the case of Heidler function ([10] and [8]), parameter *a* of the CBC function should be greater than 1, $a > 1$.

Parameter *b* determines the shape of the decreasing part of the function and thus the decreasing time to half of the peak value. It mostly determines charge transfer of the return stroke current at the channel base. For the proposed CBC function charge transfer is calculated analytically as the following:

$$q = \int_0^t i(t)\,\mathrm{d}t = \begin{cases} \dfrac{\mathrm{Q}_0\mathrm{e}^a}{a^{a+1}}\gamma(a+1, a\dfrac{t}{t_m}), & 0 \le t \le t_m, \\ \dfrac{\mathrm{Q}_0\mathrm{e}^a}{a^{a+1}}\gamma(a+1,a) + & \\ + \dfrac{\mathrm{Q}_0\mathrm{e}^b}{b^{b+1}}\left[\gamma(b+1, b\dfrac{t}{t_m}) - \gamma(b+1,b)\right], & t_m \le t \le \infty, \end{cases} \tag{6}$$

where: $\mathrm{Q}_0 = I_m t_m$ and $\gamma(a+1,x) = \int_0^x t^a\,\mathrm{e}^{-t}\,\mathrm{d}t$ – the incomplete $\gamma-$function (Euler function of the second kind).

For chosen parameter *a*, parameter *b* can be determined so to obtain desired charge transfer. For example in [10], for the maximum value of return stroke channel-base current $I_m = 13\,\mathrm{kA}$ and rise time to peak $t_m = 0.5\,\mu\mathrm{s}$, the chosen charge transfer is $q = 50\,\mathrm{mC}$. With here proposed CBC function approximate values of charges transferred up to $t_m = 0.5\,\mu\mathrm{s}$, for different values of parameter *a*, are calculated as following: $q_1 = 4.78\,\mathrm{mC}$ for $a_1 = 0.9$, $q_2 = 4.84\,\mathrm{mC}$ for $a_2 = 0.85$, $q_3 = 5.03\,\mathrm{mC}$ for $a_3 = 0.7$ and $q_4 = 5.25\,\mathrm{mC}$ for $a_4 = 0.55$. It means that the value of *b* must be determined, for corresponding value of *a*, such that the total charge transfer is $q = 50\,\mathrm{mC}$ for $t \to \infty$, but practically already for $t = 100\,t_m$. If calculated for each example, the following values are obtained for parameter *b*: for $a_1 = 0.9 \Rightarrow b_1 = 0.1953$, for $a_2 = 0.85 \Rightarrow b_2 = 0.1956$, for $a_3 = 0.7 \Rightarrow b_3 = 0.1967$, for $a_4 = 0.55 \Rightarrow b_4 = 0.1979$.

Calculations for $\gamma-$functions are done by Mathematica program package, but also using Fortran program and expression (6).

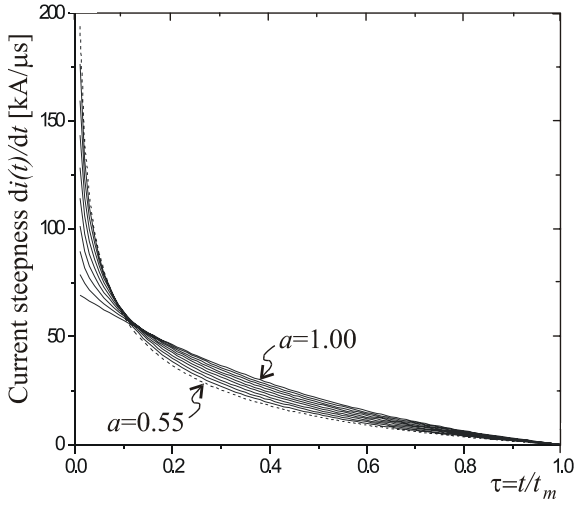

Fig.3 - *Current steepness for different values of a starting from dash line with a*=0.55 *to* 1.00, *with step* 0.05, *with decreasing concaveness, versus* τ.

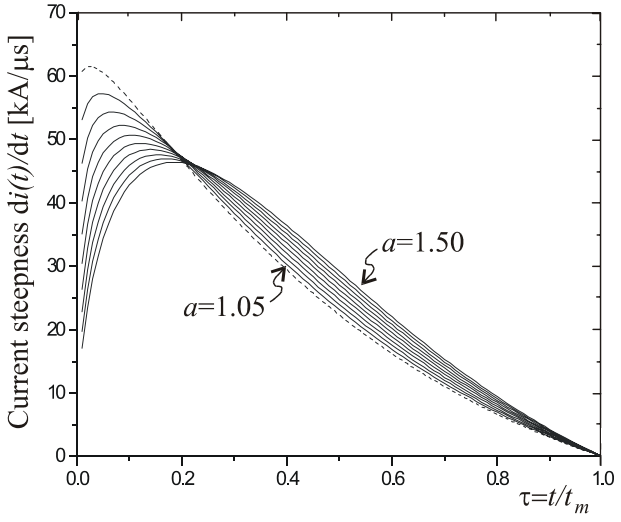

Fig.4 - *Current steepness for different values of a starting from dash line with a*=1.05 *to* 1.50, *with step* 0.05, *with decreasing maximum for increasing values of* τ.

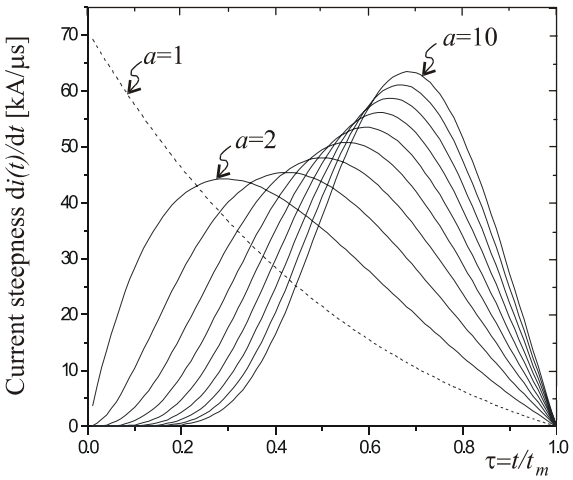

Fig. 5 - *Current steepness for different values of a starting with* a=1 *to* 10, *with step* 1, *from dash line, with increasing maximum for increasing values of* τ.

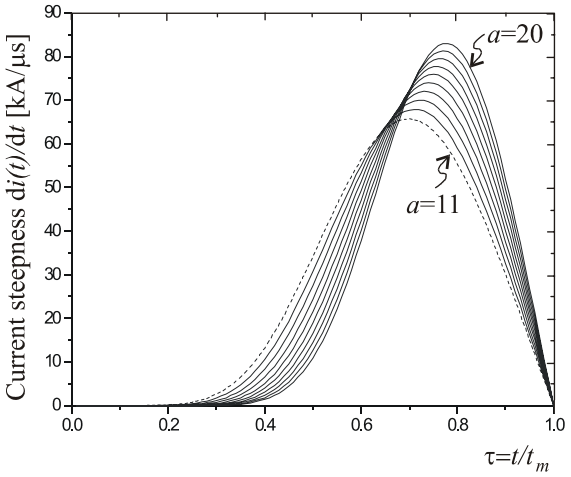

Fig.6 - *Current steepness for different values of a starting from dash line, with* a=11 *to* 20, *with step* 1, *with increasing maximum for increasing values of* τ.

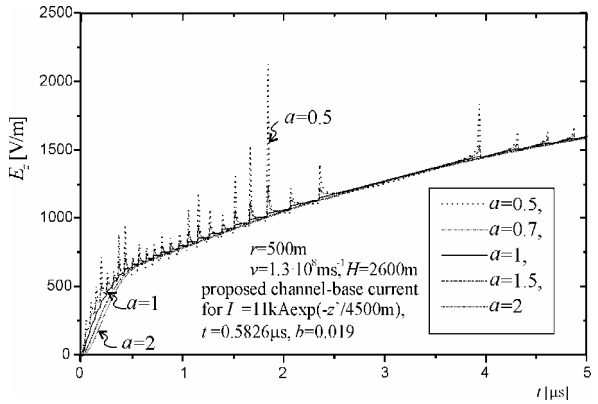

Fig.7 - E_z *component, for* $r = 500\,\mathrm{m}$ *and* $z = 0$, *for first* $5\,\mu\mathrm{s}$, *for b=0.019 and for different values of a.*

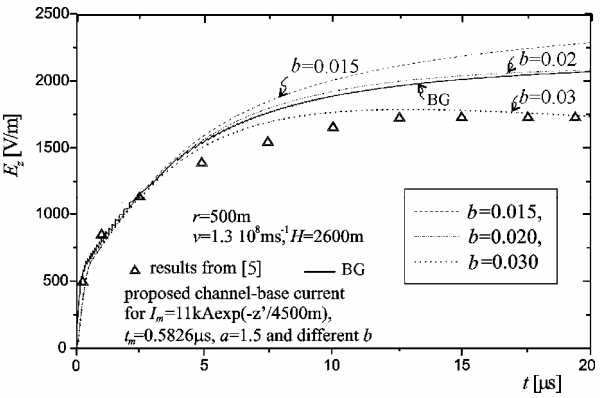

Fig.8 - E_z *component for* $r = 500\,\mathrm{m}$ *and* $z = 0$ *for first* $20\,\mu\mathrm{s}$, *for a*=1.5 *and for different values of b.*

Some comments on the CBC parameters choice

The function chosen for the lightning return stroke channel-base current is:

- continuous, as well as its first derivative;
- simple and integrable;
- can be convex or concave in the rising part;
- can have different desired current steepness;
- can give desired charge transfer;
- can have chosen time of decreasing to half of the peak value;
- can have chosen rising time and
- maximum value of the current, without peak correction factor.

It can follow convex shape of the BG function, but very high values of the first derivative at $t = 0^+$ give unrealistic spikes in the results for the field. This was analyzed and presented in Fig.7 for the points at the distance *r*=500m at the surface of perfectly conducting ground. Parameter *a* has to be greater than 1, in order to avoid these spikes. In that case the function has convex to concave shape and the saddle point in the rising part, which gives smooth shape of the field functions depending also on the number of antenna segments and discretization in time used during numerical calculations.

Often used Heidler function has the same shape in the rising part, but it is not analytically integrable. It has the peak correction factor, so as some other proposed functions, as "pulse function" in [8]. In here proposed function there is no need for the peak correction factor as the peak value is exactly I_m. Value of the parameter *b* is analyzed in Fig.8. For greater *b* decreasing time to half of the peak value is shorter and the results for field at $r = 500\,\mathrm{m}$ tend to the results (SMR) from [5], as the current decays faster from the maximum for that function than for the BG function. If *a*=1.5 is chosen for the proposed function parameter, then *b*=0.02 would give better results compared to (BG), but *b*=0.03 compared to the (SMR) results from [5].

The results for LEMF components presented in Figs.9-18 are calculated for the following parameters: $r_0 = 5\,\mathrm{cm}$ for the radius of the channel, $H = 2600\,\mathrm{m}$ for the height of the channel, $v = 1.3 \cdot 10^8\,\mathrm{ms}^{-1}$ for the current-wave propagation speed, $I_m = 11\mathrm{kA}$, $t_m = 0.5826\mu\mathrm{s}$, *a*=1.5, *b*=0.02 and *b*=0.03, $P(z') = \exp(-z'/\lambda)$ as an attenuation factor, with the constant $\lambda = 4500\,\mathrm{m}$, as an average value to have the results comparable with those from [5], where the current is assumed to be both attenuated and distorted along the channel.

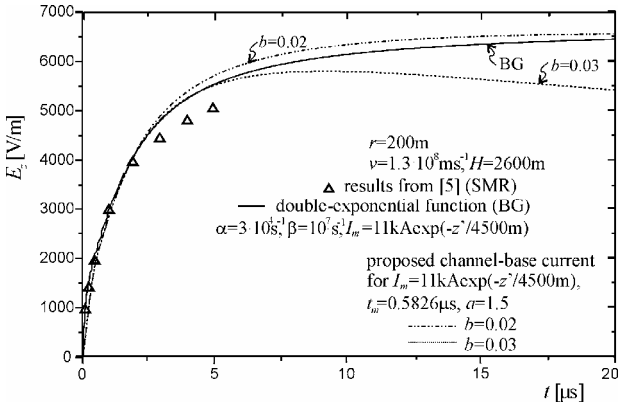

Fig.9 - E_z *component for* $r = 200\,\mathrm{m}$ *and* $z = 0$.

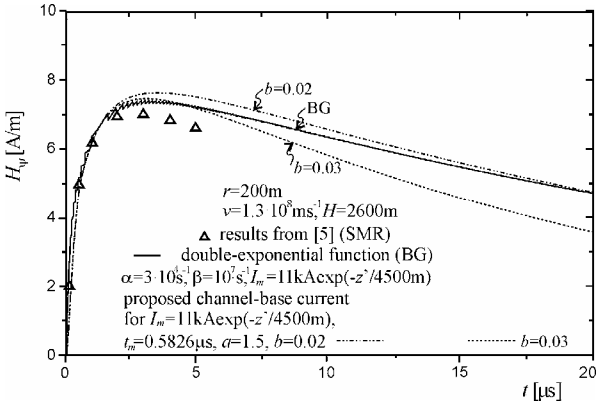

Fig.10 - H_ψ *component for* $r = 200\,\mathrm{m}$ *and* $z = 0$.

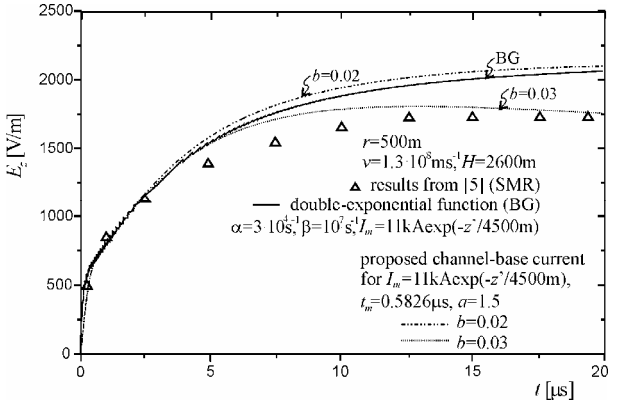

Fig.11 - E_z *component for* $r = 500\,\mathrm{m}$ *and* $z = 0$.

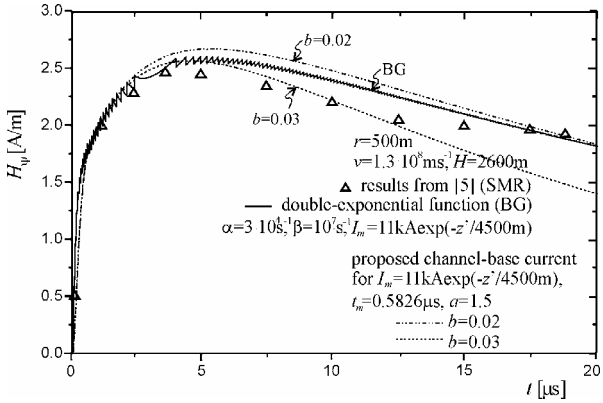

Fig.12 - H_ψ *component for* $r = 500\,\mathrm{m}$ *and* $z = 0$.

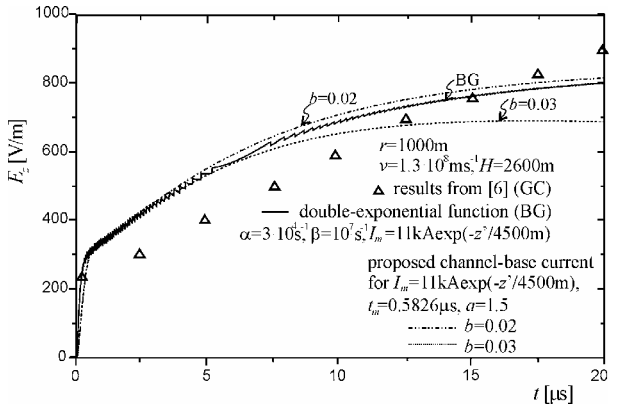

Fig.13 - E_z *component for* $r = 1000\,\mathrm{m}$ *and* $z = 0$.

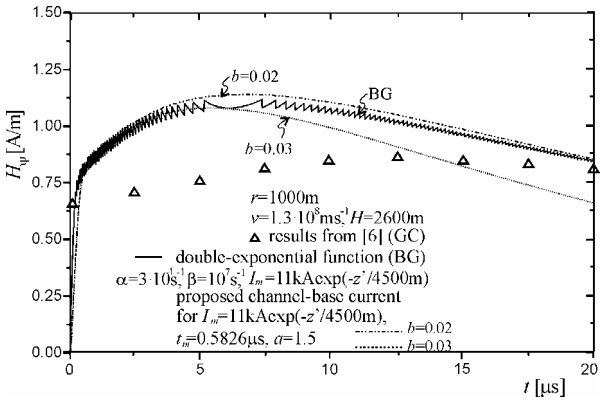

Fig.14 - H_ψ *component for* $r = 1000\,\mathrm{m}$ *and* $z = 0$.

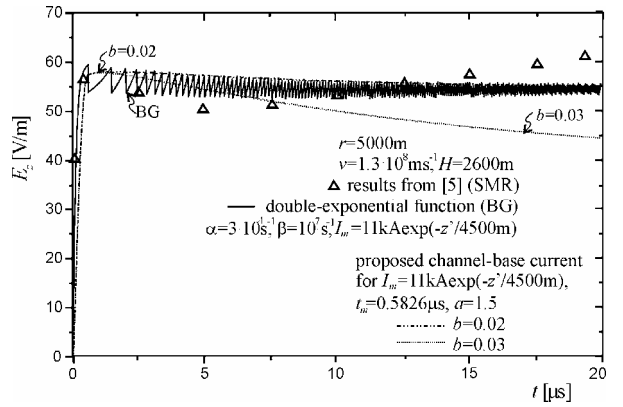

Fig.15 - E_z *component for* $r = 5000\,\mathrm{m}$ *and* $z = 0$.

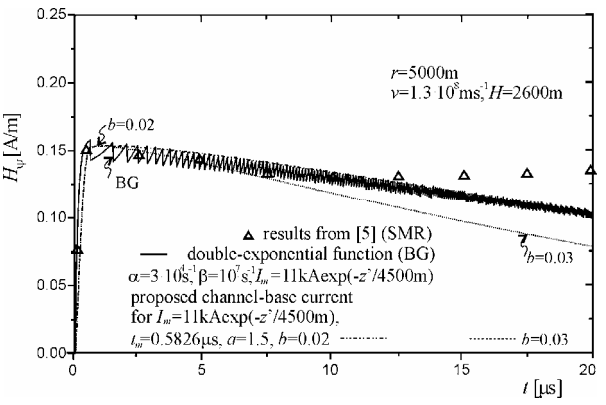

Fig.16 - H_ψ *component for* $r = 5000\,\mathrm{m}$ *and* $z = 0$.

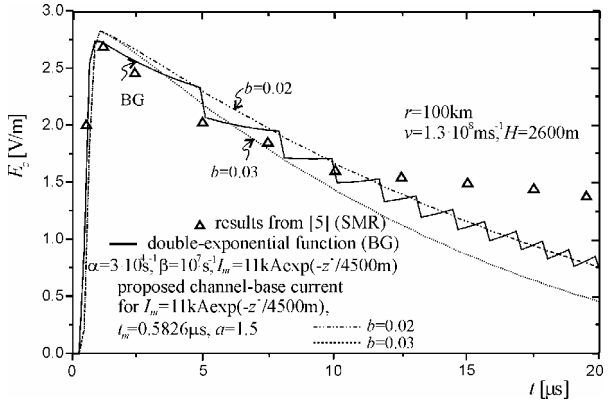

Fig.17 - E_z *component for* $r = 100\,\text{km}$ *and* $z = 0$.

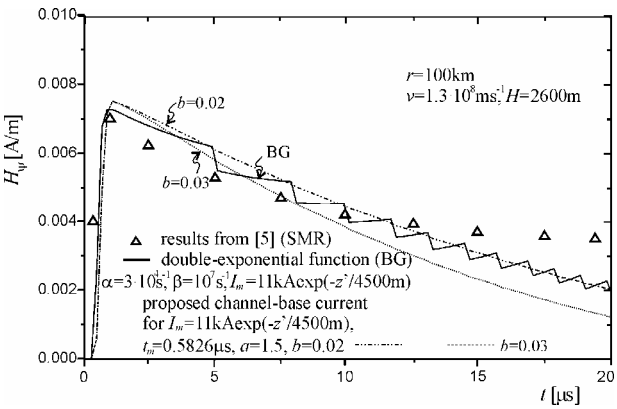

Fig.18 - H_ψ *component for* $r = 100\,\text{km}$ *and* $z = 0$.

Figs.9-18 present comparison of the results using the proposed CBC function, calculated (BG) results for the BG function as channel-base current, the results from [5] (SMR) and [6] (GC). There is a good agreement of the results. The results for electric and magnetic field at the ground surface point, for $r = 200\,\text{m}$, are presented in Figs.9 and 10, for $r = 500\,\text{m}$ in Figs.11 and 12, for $r = 1000\,\text{m}$ in Figs.13 and 14, for $r = 5000\,\text{m}$ in Figs.15 and 16, and for $r = 100\,\text{km}$ in Figs.17 and 18.

It should be noticed that for greater distances comparison to SMR results shows better agreement for the first $10\,\mu\text{s}$ than later, as the consequence of proposed function decaying faster than of the function used in [5], which after fast decaying to the half of the peak value, later decays very slow.

The influence of the total lightning channel height on LEMF

The influence of the total lightning channel height on the values of LEMF components is presented in this section. For obtaining numerical results, the following parameters for CBC are chosen: $I_m = 11\text{kA}$, $t_m = 0.5826\mu\text{s}$, a=1.5, b=0.02, $P(z') = \text{e}^{-z'/\lambda}$ and $\lambda = 4500\,\text{m}$. Parameters of the function are chosen so that it approximates BG function with parameters $I_m = 11\text{kA}$, $t_m = 0.5826\mu\text{s}$, $\alpha = 3\cdot10^4\,\text{s}^{-1}$, $\beta = 10^7\,\text{s}^{-1}$. The results are obtained using the same procedure for both of the functions.

LEMF components at different distances from the channel base are presented in the following figures, for $v = 1.3\cdot10^8\,\text{ms}^{-1}$ as the current-wave propagation speed along the channel, for different equivalent lightning channel heights: H = 2600 m, 4500m, 7000 m and 12000m. Vertical electric field component at ground surface points (z=0) for r=30m from the channel-base is presented in Fig.19 and for r=50m in Fig.21. On these distances lightning channel height has great influence on vertical electric field values. Vertical electric field at the distance r=500m from the channel base (in Fig.23) does not differ a lot for different lightning channel heights, but changes the function shape after $\approx 30\,\mu\text{s}$ if the channel height is shorter than about 3500m.

Results for azimuthal magnetic field component, H_ψ, for the distances r=30m, 50m and 500m, for different lightning channel heights are presented in Figs.20, 22 and 24. It can be noticed that magnetic field is almost the same for different channel heights for the near zone, and is only slightly greater short after the maximum value in the case of longer channel. For greater distances from the channel base, calculated for the points at ground surface, for each lightning channel height there is a spike in a certain time moment. The results for vertical electric field at the ground surface points for r=1km and 5km are presented in Figs.25 and 27. They show that for these distances the influence of the channel height on vertical electric field values is smaller than in near zone, as well as on azimuthal magnetic field (Figs.26 and 28 for r=1km and 5km), but there are spikes in certain time moments.

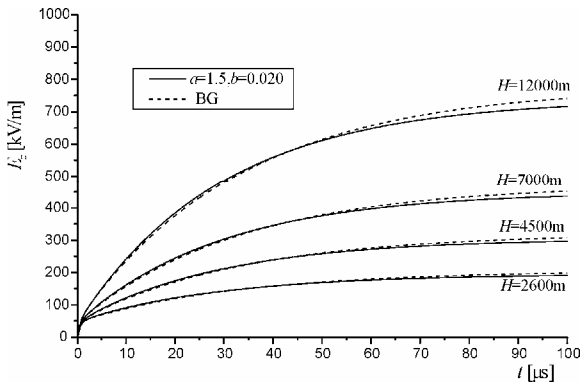

Fig. 19 - *Electric field component* E_z *for* r=30m *and* z=0.

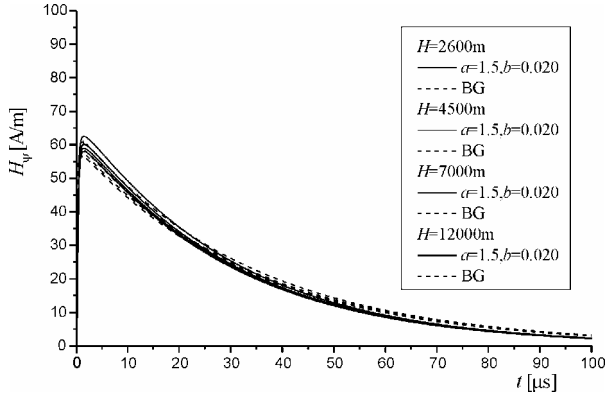

Fig.20 - *Magnetic field component* H_ψ *for* r=30m *and* z=0.

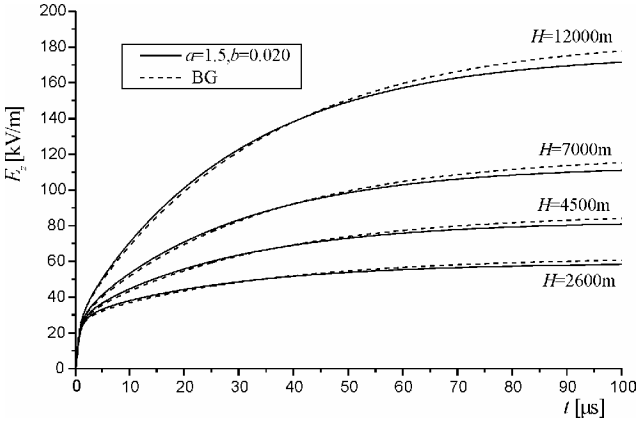

Fig.21 - *Electric field component* E_z *for* r=50m *and* z=0.

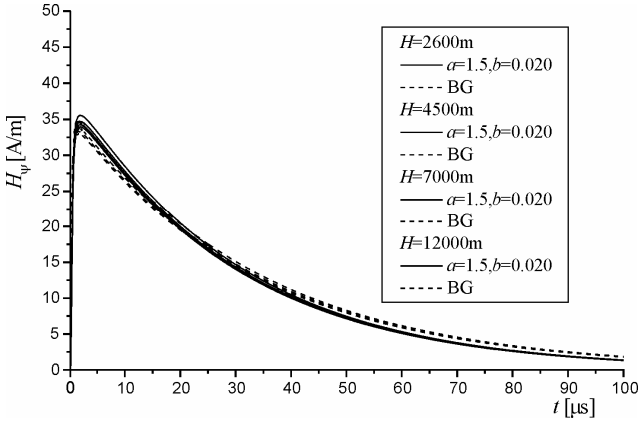

Fig.22 - *Magnetic field component* H_ψ *for* r=50m *and* z=0.

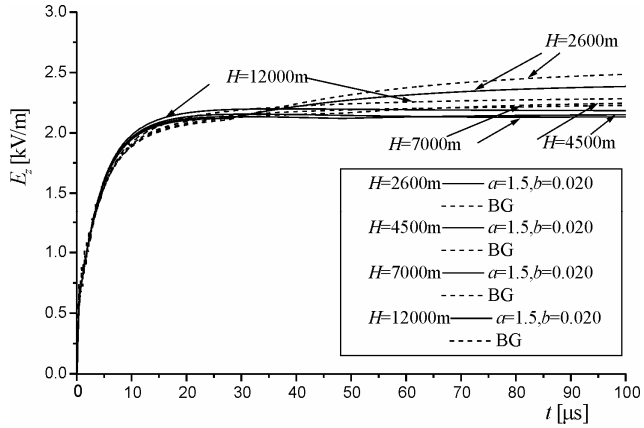

Fig.23 - *Electric field component* E_z *for* r=500m *and* z=0.

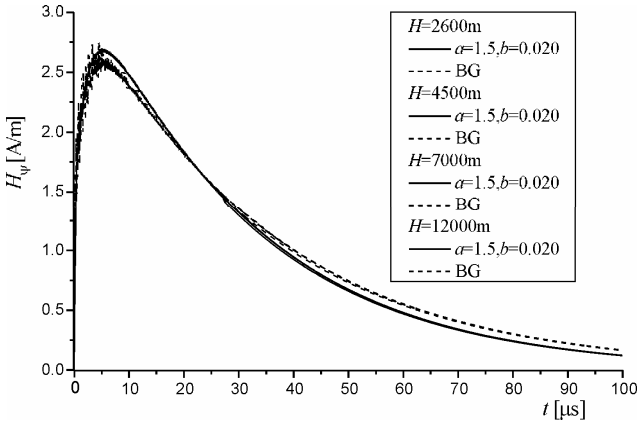

Fig.24 - *Magnetic field component* H_ψ *for* r=500m *and* z=0.

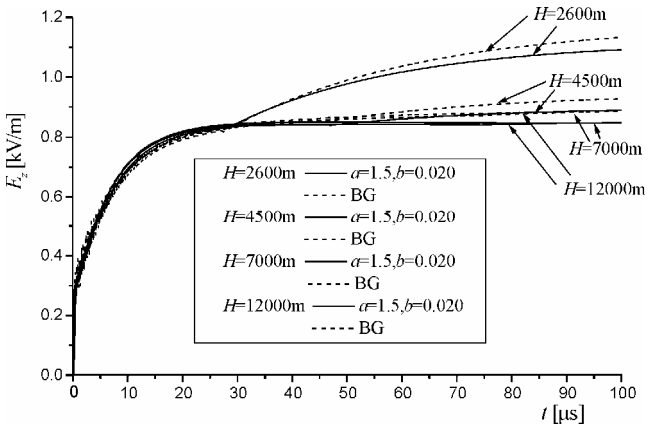

Fig.25 - *Electric field component* E_z *for* r=1km *and* z=0.

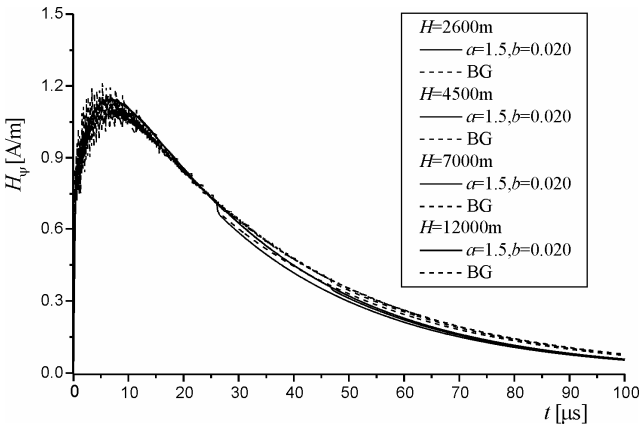

Fig.26 - *Magnetic field component* H_ψ *for* r=1km *and* z=0.

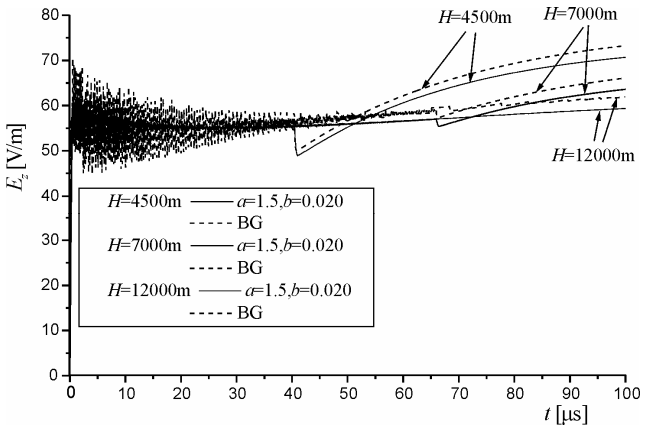

Fig.27 - *Electric field component* E_z *for* r=5km *and* z=0.

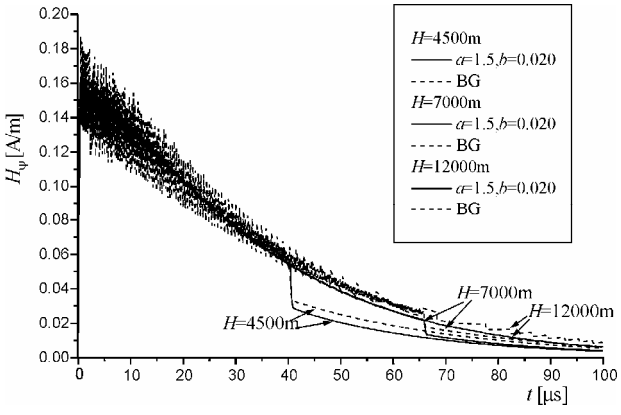

Fig.28 - *Magnetic field component* H_ψ *for* r=5km *and* z=0.

CALCULATING LEMF IN FREQUENCY DOMAIN

Theoretical approach

One model for numerical determining of electromagnetic field structure in frequency domain is used in this paper as the basis for modeling of electromagnetic field radiated during lightning discharge at the real ground. The following is adopted for the modeling procedure: lightning channel is modeled by a vertical monopole mast antenna; lightning return stroke current at the base of the channel, as an excitation, is modeled by a pulse $\delta-$generator of voltage *U* and frequency *f* ; and the real ground is treated as homogeneous lossy half-space of known electrical parameters.

This model of the lightning discharge is used in order to include the influence of finite conductivity of the real ground. The structure of LEMF in time domain can be obtained afterwards using FFT. This kind of modeling is done because including real ground influence would be more complicated in calculations directly in time domain ([4], [7]).

A few steps are made in the procedure of obtaining general model. The first step is to adopt thin wire antenna model of the lightning discharge channel. Then, for the chosen frequency $f \in [0.01 \div 10\,\mathrm{MHz}]$, the Unknown Current Distribution (UCD) along the antenna is determined. Because of the wide range of frequencies of interest, the total height of the antenna is divided into segments for higher frequencies, while UCD-s of each segment satisfy conditions of current continuity at the ends/beginnings of segments and also current's first derivative continuity. The next step is to calculate electromagnetic field components in arbitrary field point in the air as the function of frequency, using definition relations.

UCD-s along the antenna are numerically determined using the Moments Method (MoM) for solving integral equations for the currents. System of integral equations of two potentials (SIE-TP) is used in this paper ([12]). Entire-domain polynomial approximation ([13]) is used for the UCD-s along the antenna segments with unknown complex current coefficients, which are determined by the Point Matching Method ([14]). Excitation is modeled by a voltage $\delta-$generator located at the base of antenna, but all of the results in this paper are referred to the potential at the beginning of first segment V_{e1}, taken as $\mathrm{V}_{e1} = U + \mathrm{V}_{ground} = 1\mathrm{V}$.

The influence of finite ground conductivity is taken into account through Sommerfeld's integral kernel (SIK) in the relations for potentials (Hertz's vector potential and electrical scalar potential) and it is modeled in a new and simple way ([15]). This model of SIK gives solution of satisfactory accuracy in a certain range of distances from the antenna without limitations for ground electrical parameters values or antenna height. The model can be used in a wide range of electrical parameters ($\varepsilon_{r1} \in [0,81]$, $\sigma_1 \in [0,\infty]$, $\mu_1 = \mu_0$). This is particularly important for the higher frequencies. The results in frequency domain are compared to the results from literature [13] and some to the results of available program packages for solving antenna problems above perfect ground [16]. The reliability of the results is analyzed in order to obtain field components in time domain using Fast Fourier Transform.

The lightning current channel is approximated by vertical mast antenna above real ground, as illustrated in Fig.29. The problem of lightning generated electromagnetic field can be solved if unknown current distribution along the antenna is determined. Antenna having total length *h* is divided into *N* segments, each of length l_k, such that $h = l_1 + l_2 + \ldots + l_N$. Thin wire approximation is used if radius $a << l_k$ and $a << \lambda_0$ (λ_0-wavelength in the air). Antenna is excited in its base by the $\delta-$generator of voltage *U* and frequency f.

Entire-domain polynomial approximation is used, so the UCD along the axis of the $k-$th segment is

$$\underline{I}_k(s_k') = \sum_{m=0}^{M_k} \underline{\mathrm{I}}_{mk} (s_k'/l_k)^m, 0 \le s_k' \le l_k, z_k' = z_{\mathrm{A}k} + s_k',$$

where $z_{\mathrm{A}k}-$the beginning of the $k-$th segment, and $\underline{\mathrm{I}}_{mk}$, $m = 0,1,2,\ldots,M_k$, the unknown current complex coefficients. Distributed impedance along the $k-$th segment is $\underline{Z}_k'(s_k') = \mathrm{const}$, for $k = 1,2,\ldots,N$. The upper half-space is the air with electrical parameters ε_0, μ_0 and $\sigma_0 = 0$, and the lower half-space is ground, treated as linear, isotropic and homogeneous medium, with known parameters $\varepsilon_1 = \varepsilon_{r1}\varepsilon_0$, $\mu_1 = \mu_0$ and σ_1. Complex conductivity is defined as $\underline{\sigma}_i = \sigma_i + \mathrm{j}\omega\varepsilon_i$, for $\omega = 2\pi f$, and complex propagation constant as $\underline{\gamma}_i = \alpha_i + \mathrm{j}\beta_i = \sqrt{\mathrm{j}\omega\varepsilon_i\,\underline{\sigma}_i}$, for *i*=0,1. The refraction index is $\underline{n}_{10} = \underline{\gamma}_1 / \underline{\gamma}_0 = \sqrt{\underline{\varepsilon}_{r1}} = \sqrt{\varepsilon_{r1} - \mathrm{j}60\sigma_1\lambda_0}$.

System of integral equations of two potentials(SIE-TP)

The SIE-TP can be used for solving different wire antenna and grounding problems ([12]).

Using general formulation of the SIE-TP different excitation models can be included and also distributed or coating impedances of the antenna. The SIE-TP can be written for any wire structure in the presence of inhomogeneous medium if:

- excitation of the wire structure is harmonic generator;
- inhomogeneity can be modeled with a finite number of homogeneous domains;
- it is possible to determine the total tangential component of Hertz's vector and electrical scalar potential at the surface of the $n-$th conductor in the domain where the $n-$th conductor of the wire structure is positioned.

The SIE-TP can be written in the following implicit form

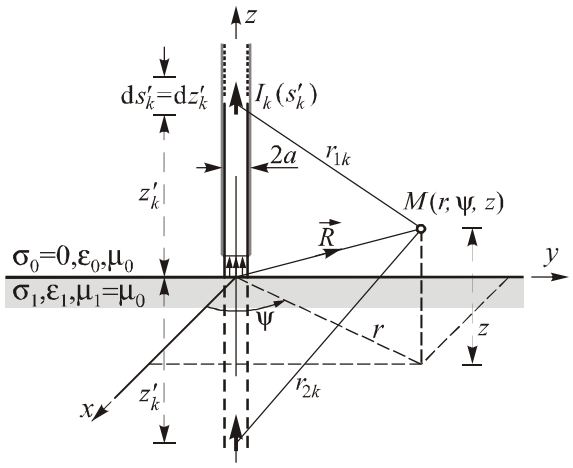

Fig.29 - *Antenna model and geometry of the problem in the case of the real ground.*

$$\underline{\gamma}_0 \int_{s=0}^{s_n} \varphi_0(s)\,\mathrm{ch}\left[\underline{\gamma}_0(s_n-s)\right]\mathrm{d}s + \underline{\gamma}_0^{\,2} \int_{s=0}^{s_n} \Pi_{z0}(s)\,\mathrm{sh}\left[\underline{\gamma}_0(s_n-s)\right]\mathrm{d}s +$$

$$+ \int_{s=0}^{s=s_n} \underline{Z}_n'\,\underline{I}_n(s)\,\mathrm{sh}\left[\underline{\gamma}_0(s_n-s)\right]\mathrm{d}s =$$

$$= \underline{V}_{en}\,\mathrm{sh}\left(\underline{\gamma}_0 s_n\right) + \int_{s=0}^{s=s_n} \left(\vec{E}_{exn}\cdot\hat{s}_n\right)\mathrm{sh}\left[\underline{\gamma}_0(s_n-s)\right]\mathrm{d}s, \qquad (7)$$

$$\varphi_0(s_n) + \underline{\gamma}_0 \int_{s=0}^{s_n} \varphi_0(s)\,\mathrm{sh}\left[\underline{\gamma}_0(s_n-s)\right]\mathrm{d}s + \underline{\gamma}_0^{\,2} \int_{s=0}^{s_n} \Pi_{z0}(s)\,\mathrm{ch}\left[\underline{\gamma}_0(s_n-s)\right]\mathrm{d}s +$$

$$+ \int_{s=0}^{s=s_n} \underline{Z}_n'\,\underline{I}_n(s)\,\mathrm{ch}\left[\underline{\gamma}_0(s_n-s)\right]\mathrm{d}s =$$

$$= \underline{V}_{en}\,\mathrm{ch}\left(\underline{\gamma}_0 s_n\right) + \int_{s=0}^{s=s_n} \left(\vec{E}_{exn}\cdot\hat{s}_n\right)\mathrm{ch}\left[\underline{\gamma}_0(s_n-s)\right]\mathrm{d}s, \qquad (8)$$

where: $\varphi_0(s)$ and $\Pi_{z0}(s)$ are electrical scalar potential and the resulting tangential component of Hertz's vector potential, calculated at the surface of the $n-$th segment, respectively, $\underline{V}_{en}$ – the unknown integration constant, i.e. potential at the beginning of the $n-$th segment, $\vec{E}_{exn}$ – external electric field, and s_n – local coordinate along the generatrice of the $n-$th segment and $0 \le s \le s_n \le l_n$, for $n = 1,2,...,N$.

The Hertz's vector potential in arbitrary field point in the air is $\vec{\Pi}_0(\vec{r}) = \Pi_{z0}\hat{z}$, and calculated at the surface of the $n-$th segment it can be expressed as

$$\Pi_{z0}(s_n) = \frac{1}{4\pi\underline{\sigma}_0} \sum_{k=1}^{N} \int_{s_k'=0}^{l_k} I_k(s_k')\left[K_0(r_{1k}) + S_{00}^{\,v}(r_{2k})\right]\mathrm{d}s_k', \qquad (9)$$

and electrical scalar potential,

$$\varphi_0(\vec{r}) = -\mathrm{div}\,\vec{\Pi}_0 = -\partial\Pi_{z0}/\partial z,$$

can be expressed as

$$\varphi_0(s_n) = \frac{1}{4\pi\underline{\sigma}_0} \sum_{k=1}^{N} \int_{s_k'=0}^{l_k} I_k(s_k')\frac{\partial}{\partial s_k'}\left[K_0(r_{1k}) - S_{00}^{\,v}(r_{2k})\right]\mathrm{d}s_k', \qquad (10)$$

where: r_{1k}, r_{2k} – the distances from the current element and its image to the matching point, respectively; $K_0(r_{1k}) = \exp(-\underline{\gamma}_0 r_{1k})/r_{1k}$ the standard form of the potential kernel of the current element and $S_{00}^{\,v}(r_{2k})$ the Sommerfeld's integral, i.e. semi-infinite integral with a very complex integrand,

$$S_{00}^{\,v}(r_{2k}) = \int_{\alpha=0}^{\infty} \widetilde{R}_{z10}(\alpha)\,\widetilde{K}_0(\alpha, r_{2k})\,\mathrm{d}\alpha, \qquad (11)$$

where: $\widetilde{R}_{z10}(\alpha) = \widetilde{R}_{z10}(u_0) = (\underline{n}_{10}^{\,2}u_0 - u_1)/(\underline{n}_{10}^{\,2}u_0 + u_1)$ is the spectral reflection coefficient (SRC), for the values $u_0 = \sqrt{\alpha^2 + \underline{\gamma}_0^{\,2}}$, $u_1 = \sqrt{\alpha^2 + \underline{\gamma}_1^{\,2}} = \sqrt{u_0^{\,2} + \underline{\gamma}_0^{\,2}(\underline{n}_{10}^{\,2} - 1)}$, and $\widetilde{K}_0(\alpha, r_{2k})$ – the spectral form of the standard potential kernel from the image in flat mirror,

$$K_0(r_{2k}) = \int_{\alpha=0}^{\infty} \widetilde{K}_0(\alpha, r_{2k})\,\mathrm{d}\alpha =$$

$$= \int_{\alpha=0}^{\infty} \frac{\exp[-u_0(z+z_k')]}{u_0}\alpha J_0(\alpha r)\,\mathrm{d}\alpha = \exp(-\underline{\gamma}_0 r_{2k})/r_{2k}, \qquad (12)$$

where: $r_{1k} = \sqrt{r^2 + (z - z_k')^2}$, $r_{2k} = \sqrt{r^2 + (z + z_k')^2}$, and $J_0(\alpha r)$ – the Bessel's function of the first kind and zero order.

Simple new approximate model for the SRC is used in this paper, as in [15]. The SRC approximation is expressed as

$$\widetilde{R}_{z10}(u_0) \cong B + A(\underline{\gamma}_0/u_0), \qquad (13)$$

where A and B are the constants that can be determined matching (13) in the points $u_0 = \underline{\gamma}_0$ and $u_0 \to \infty$.

The following values are obtained for the constants:

$$B = \widetilde{R}_{z10}(u_0 \to \infty) = (\underline{n}_{10}^{\,2} - 1)\big/(\underline{n}_{10}^{\,2} + 1) \qquad (14)$$

and

$$A = (\underline{n}_{10} - 1)/(\underline{n}_{10} + 1) - B. \qquad (15)$$

Substituting (13) in (11), approximate solution of the Sommerfeld's integral is obtained

$$S_{00}^{\,v}(r_{2k}) \cong BK_0(r_{2k}) + A\underline{\gamma}_0 L(r_{2k}), \qquad (16)$$

where $L(r_{2k})$ is the new integral kernel, as in [15].

In this paper SRC is approximated by coefficient B and better approximation of SRC using also coefficient A and consequently both terms of expression (16) is going to be used in further investigations.

Numerical model description

Explicit form of the SIE-TP for UCD-s is obtained if (16) is substituted in (9) and (10), and then those in (7) and (8). The unknown integration constants V_{en}, $n = 1, 2, ..., N$, are: $V_{e1} = U + V_{ground} = 1\text{V}$, and the rest $(N-1)$ satisfy $N-1$ conditions for the potential continuity at the joints of the segments. The UCD-s along segments are approximated by polynomials, so there are $N_u = \sum_{k=1}^{N} (1 + M_k)$ unknown current coefficients, which are determined as solution of algebraic equations system obtained by matching SIE-TP (7) in N_u points ([14]).

Input admittance Y_{ul} and input impedance Z_{ul}, referred to the potential of excitation point V_{e1}, are defined by the following relation

$$Y_{ul} = G_{ul} + jB_{ul} = 1/Z_{ul} = I_1(0^+)/V_{e1}. \qquad (17)$$

On the basis of this numerical model program package in FORTRAN is realized for the PC numerical calculations. In order to check the reliability of the model many numerical experiments were made and some results are presented in the following paragraph.

Numerical examples

The results for the input resistance and reactance for $h = \lambda_0/2$ and $h = \lambda_0/4$ monopole having radius $a = 0.007022\lambda_0$, above real ground, for different values of ε_{r1}, versus $\sigma_1\lambda_0$, for *M*=3 as the current approximation polynomial degree, are presented in Figs.30-33. The results for the input conductance/susceptance for $h = 300\,\text{m}$, $R' = 0.1\Omega/\text{m}$, $N = 30$, $l_k = 10\,\text{m}$, $M_k = 3$, $k = 1,..., N$, for $\varepsilon_{r1} = 10$ and $\sigma_1 = 0.01\text{S/m}$, versus frequency, in the frequency range $0.01 \div 2\,\text{MHz}$, are presented in Figs.34-35 and for the input resistance/reactance in Figs.36-37. Graphics are obtained for the frequency step $\Delta f = 10\,\text{kHz}$. For the antenna parameters $h = 300\,\text{m}$, $a = 0.05\,\text{m}$, N=30 segments, polynomial degree $M_k = 3$, $k = 1,..., 30$ and $f = 3\,\text{MHz}$, the results for the real and imaginary part of the current along the antenna versus z'/h are presented in Figs.38-39 for ground parameters $\varepsilon_{r1} = 2$ and 10, for $\sigma_1 = 10^{-1}\,\text{S/m}$ and $\sigma_1 = 10^{-5}\,\text{S/m}$. For the polynomial degree M_k of $k-$th segment current approximation it is usually enough to choose $2 \le M_k \le 4$ for the segment length $l_k \le 0.50\lambda_0$. In the case of a very long antenna according to the wave-length, as for the part of lightning discharge spectrum frequencies, the approximation of lightning channel current, the antenna should be divided into segments of length $l_k \le 0.50\lambda_0$, and the conditions $a << l_k$ and $a << \lambda_0$ should also be satisfied.

The results for electric field components E_z and E_y, for frequency $f = 3\,\text{MHz}$, $\lambda_0 = 100\,\text{m}$, at the distances $r \le 2.5\lambda_0$ from antenna basis, at ground surface, for the antenna parameters $h = 300\,\text{m}$, $a = 0.05\,\text{m}$, number of segments $N = 20, 30$ and 50, polynomial degree $M_k = 3$, $k = 1, 2, ..., N$, for real ground parameters $\varepsilon_{r1} = 10$ and $\sigma_1 = 0.01\text{S/m}$, are presented in Figs.40-41. E_x component of the electric field at ground level is equal to zero.

The results of the frequency domain analysis of vertical mast antenna above linear, isotropic and homogeneous ground for different number of antenna segments and different polynomial degree of the UCD approximation are presented. The validity of the output results (UCD and input impedance/admittance) of programs realized in FORTRAN is compared to the results from literature and other programs results ([13], [16]).

The results are presented for the antenna length of several hundreds of metres and further calculations are aimed to longer antennas (for higher frequencies) i.e. to the lightning channel heights of several thousands of km, for example the values from 2600m to 7000m often used for the lightning channel modeling. It should be noticed that for arbitrary height *h* the segmentation to *N* segments, needed for obtaining satisfactory results, depends on frequency and the segment length has to be $l_k \le \lambda_0/2$, for $k = 1,..., N$, while satisfactory polynomial degree is $M_k = 3$. Simple approximation of Sommerfeld's integral kernel is used in this paper. Coefficient that includes real ground influence can be used as $\widetilde{R}_{z10}(u_0) \cong B$, but better results can be obtained for $\widetilde{R}_{z10}(u_0) \cong B + A\underline{\gamma}_0/u_0$ which is going to be investigated in future calculations.

The influence of distributed resistance on current distribution and consequently on input admitttance/ impedance is not so great for the values of $R' < 10\Omega/\text{m}$. The results are compared to the results of program package AWAS [16].

CONCLUSION

In this paper antenna theory approach and thin wire approximation of lightning channel are used for determining LEMF in time domain. Proposed function for the return stroke channel-base current gives satisfactory results for calculating lightning electromagnetic field. Parameters of this function can be chosen so that it satisfies some of the desired characteristics of the return stroke channel-base current: maximum current value, rise-time to peak, maximum of the current steepness, charge transfer, decaying time to half of the peak value, etc. The results obtained for LEMF components at the field points at perfectly conducting ground surface for different distances from the lightning channel-base are in good agreement with the results from [5] and [6].

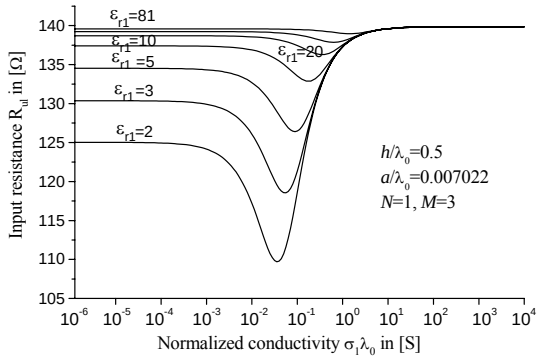

Fig.30 - *Input resistance for* $h = \lambda_0/2$ *and different* ε_{r1} *versus* $\sigma_1\lambda_0$.

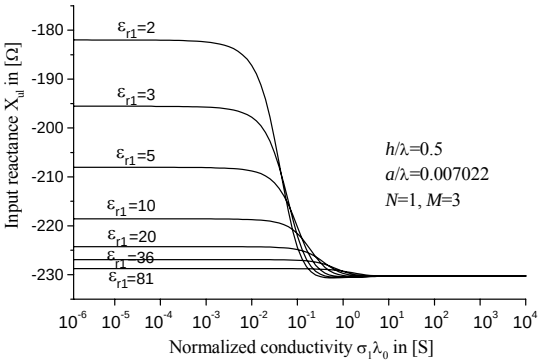

Fig.31 - *Input reactance for* $h = \lambda_0/2$ *and different* ε_{r1} *versus* $\sigma_1\lambda_0$.

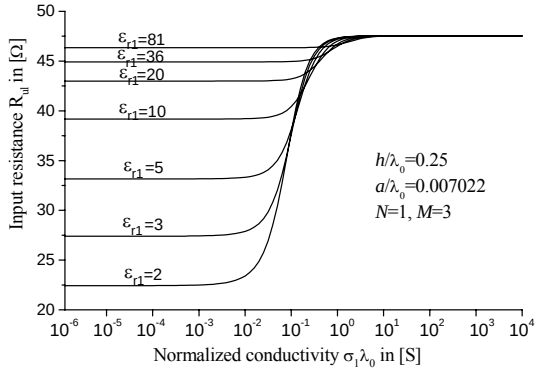

Fig.32 - *Input resistance for* $h = \lambda_0/4$ *and different* ε_{r1} *versus* $\sigma_1\lambda_0$.

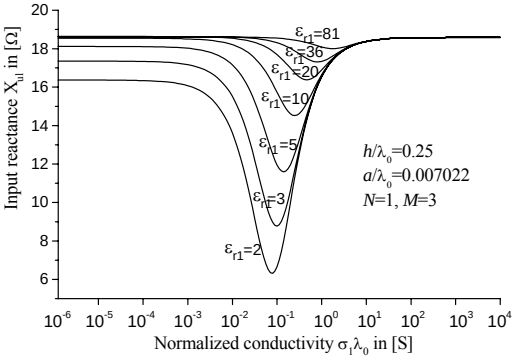

Fig.33 - *Input reactance for* $h = \lambda_0/4$ *and different* ε_{r1} *versus* $\sigma_1\lambda_0$.

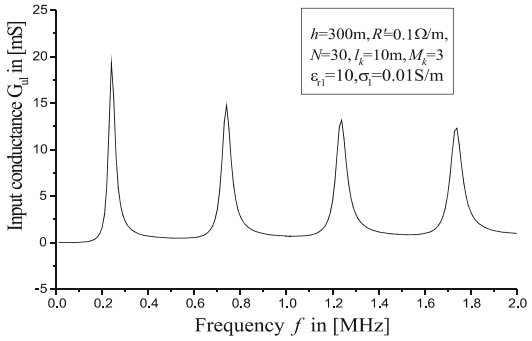

Fig.34 - *Input conductance for* $h = 300\,\text{m},\ R' = 0.1\Omega/\text{m},\ N = 30,\ l_k = 10\text{m},\ M_k = 3,\ k = 1,...,N,$ *for* $\varepsilon_{r1} = 10$ *and* $\sigma_1 = 0.01\text{S/m}$, *in the frequency range* $0.01 \div 2\,\text{MHz}$.

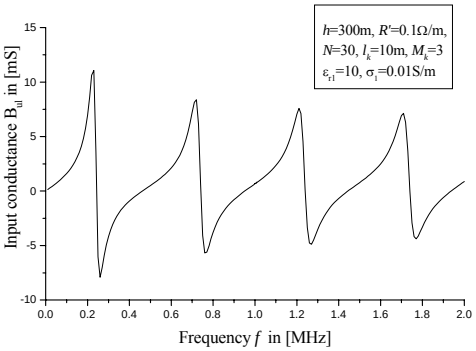

Fig.35 - *Input susceptance for* $h = 300\,\text{m},\ R' = 0.1\Omega/\text{m},\ N = 30,\ l_k = 10\text{m},\ M_k = 3,\ k = 1,...,N,$ *for* $\varepsilon_{r1} = 10$ *and* $\sigma_1 = 0.01\text{S/m}$, *in the frequency range* $0.01 \div 2\,\text{MHz}$.

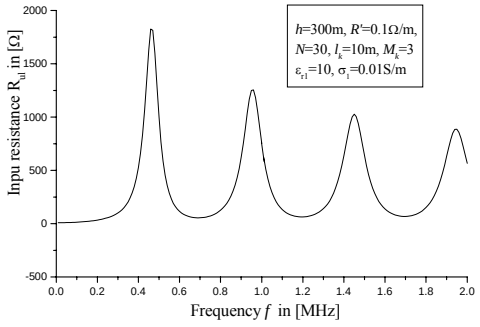

Fig.36 - *Input resistance for* $h = 300\,\text{m},\ R' = 0.1\Omega/\text{m},\ N = 30,\ l_k = 10\text{m},\ M_k = 3,\ k = 1,...,N,$ *for* $\varepsilon_{r1} = 10$ *and* $\sigma_1 = 0.01\text{S/m}$, *in the frequency range* $0.01 \div 2\,\text{MHz}$.

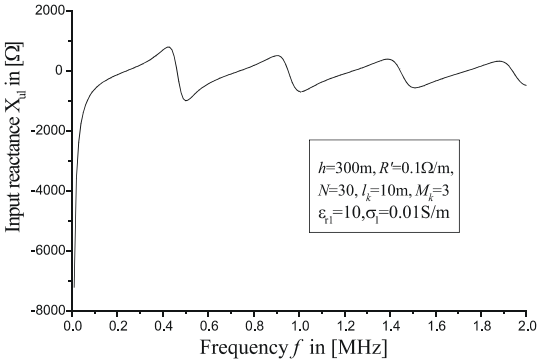

Fig.37 - *Input reactance for* $h = 300\,\text{m},\ R' = 0.1\Omega/\text{m},\ N = 30,\ l_k = 10\text{m},\ M_k = 3,\ k = 1,...,N,$ *for* $\varepsilon_{r1} = 10$ *and* $\sigma_1 = 0.01\text{S/m}$, *in the frequency range* $0.01 \div 2\,\text{MHz}$.

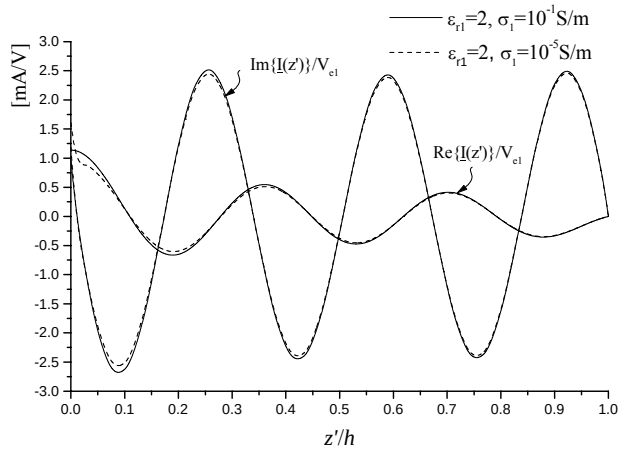

Fig.38 - *Real and imaginary part of the current versus z'/h for* $\sigma_1 = 10^{-1}$ S/m, 10^{-5} S/m; $\varepsilon_{r1} = 2$, $f = 3\,\text{MHz}$, $h = 300\,\text{m}$, $a = 0.05\,\text{m}$, $R' = 0.1\Omega/\text{m}$, $N = 30$, $M_k = 3$, $k = 1,...,30$.

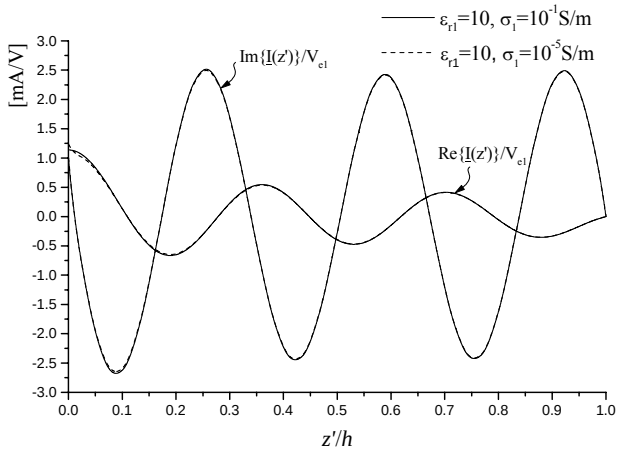

Fig.39 - *Real and imaginary part of the current versus z'/h for* $\sigma_1 = 10^{-1}$ S/m, 10^{-5} S/m; $\varepsilon_{r1} = 10$, $f = 3\,\text{MHz}$, $h = 300\,\text{m}$, $a = 0.05\,\text{m}$, $R' = 0.1\Omega/\text{m}$, $N = 30$, $M_k = 3$, $k = 1,...,30$.

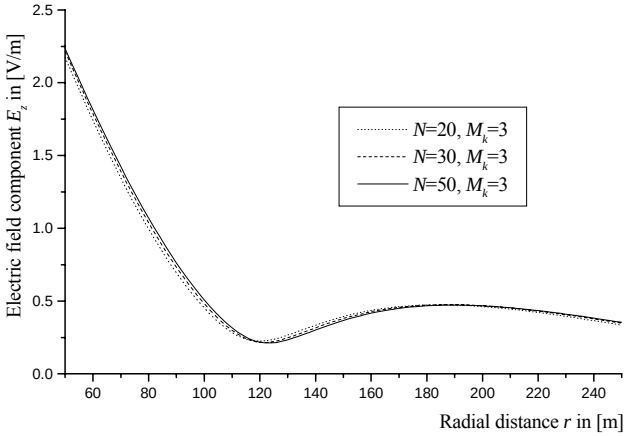

Fig.40 - E_z *component at ground surface versus r for* $f = 3\,\text{MHz}$, $h = 300\,\text{m}$, $a = 0.05\,\text{m}$, $N = 20, 30$ *and* 50, $M_k = 3$, $k = 1,...,N$, $\varepsilon_{r1} = 10$ *and* $\sigma_1 = 0.01\,\text{S/m}$.

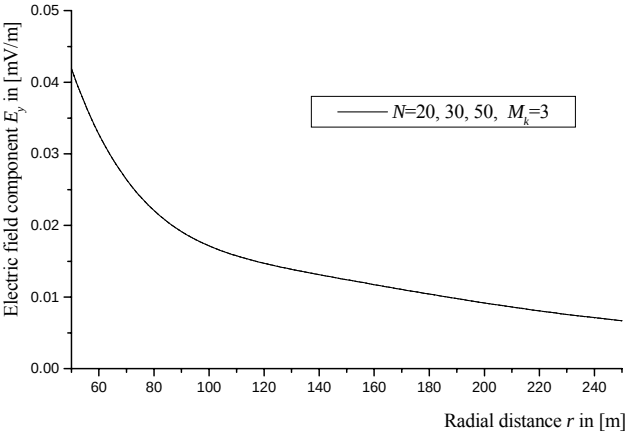

Fig.41 - E_y *component at ground surface versus r for* $f = 3\,\text{MHz}$, $h = 300\,\text{m}$, $a = 0.05\,\text{m}$, $N = 20, 30$ *and* 50, $M_k = 3$, $k = 1,...,N$, $\varepsilon_{r1} = 10$ *and* $\sigma_1 = 0.01\,\text{S/m}$.

The results for LEMF components presented in this paper show also that lightning channel height has great influence on values of electric field at ground surface points in the near zone of the channel-base. For greater distances the channel height determines a spike in a certain time moment after the onset of LEMP at the chosen distance from the channel-base to the point at ground surface. Magnetic field for the points at ground surface does not differ a lot for different lightning channel heights even for the near zone. For far zone the choice of different channel heights also produces spikes in different time moments as for electric field. For far zone the results in first $20\,\mu\text{s}$ do not differ a lot for any lightning channel height greater than 2600m. Chosen simple return stroke channel-base function and determining LEMF in time domain provide easy analysis of interrupting vertical lightning channel on a certain height from its base. Lightning is a very complicated natural process, so the assumption of vertical channel is only the first approximation that neglects branching and discharging paths inside and between the clouds.

The analysis in frequency domain including influence of the real ground electrical parameters is based on a simple new model of SRC that gave satisfactory results for EMF components. It is used for obtaining reliable general model as the basis for calculating electromagnetic field radiated by a lightning discharge at real ground in time domain using FFT, which is going to be done in further investigations.

REFERENCES

[1] V. A. Rakov, M. A. Uman: "Review and evaluation of lightning return stroke models including some aspects of their application," *IEEE Trans. on Electromagn. Compat.*, Vol.40, No.4, pp.403-426, November 1998.

[2] Y. Baba, S. Miyazaki, M. Ishii: "Reproduction of lightning electromagnetic field waveforms by engineering model of return stroke," *IEEE Trans. on Electromagn. Compat.*, Vol.46, No.1, pp.130-133, February 2004.

[3] D. Velickovic, S. Aleksic: "A new approximation of pulse phenomenon," *19th International Conference on Lightning Protection ICLP*, (distributed at the Conference), Graz, 1988.

[4] V. Javor: "Calculation of Lightning Electromagnetic Field in Time Domain: A New Return stroke Current Model, " *7th International Conference on Applied Electromagnetics PES'05*, pp.259-268, Nis, May 2005.

[5] A. Shoory, R. Moini, H. Sadeghi, V. A. Rakov: "Analysis of lightning-radiated electromagnetic fields in the vicinity of lossy ground," *IEEE Trans. on Electromagn. Compat.*, Vol.47, No.1, pp.131-145, February 2005.

[6] C. Gomes, V. Cooray: "Concepts of lightning return stroke models," *IEEE Trans. on Electromagn. Compat.*, Vol.42, No.1, pp.82-96, Feb. 2000.

[7] M. J. Master, M. A. Uman: "Transient electric and magnetic fields associated with establishing a finite electrostatic dipole," *American J. Phys.*, Vol.51, No.2, pp.118-126, February 1983.

[8] Z. Feizhou, L. Shanghe: "A new function to represent the lightning return stroke currents," *IEEE Trans. on Electromagn. Compat.*, Vol.44, No.4, pp.595-597, November 2002.

[9] R. H. Golde: "*Lightning*," Vol.1 "*Physics of lightning*," and Vol.2 "*Lightning protection*," Academic Press, London, 1977.

[10] F. Heidler, J. M. Cvetic, B. V. Stanic, *Calculation of Lightning Current Parameters*, IEEE Transactions on Power Delivery, Volume 14, No.2, April 1999, pp.399-404.

[11] V. Javor, P. D. Rancic: "Application of One Suitable Lightning Return stroke Current Model," *International Conference on Electromagnetic Compatibility EMC'06*, Barcelona, 6-9th September 2006 (paper accepted for the Conference).

[12] P. D. Rancic: "Contribution to Linear Antennas Analysis by New Forms of Integral Equations of Two Potentials," *10th Conference on the Computation of Electromagnetic Fields COMPUMAG'95, Berlin*, pp.328-329, July 1995.

[13] B. D. Popovic, M. B. Dragovic, A. R. Djordjevic: "Analysis and Synthesis of Wire Antennas," *Chichester: Willey*, 1982.

[14] R. F. Harrington: "Field Computation by Moment Methods," *NY: Macmillan*, Sec. 6.2, New York, 1968.

[15] M. P. Rancic, P. D. Rancic: "Vertical Linear Antennas in the Presence of a Lossy Half -Space: An Improved Approximate Model," *Int. J. Electron. Commun. (AEÜ)*, Vol. 60, No.5, pp.376-386, May 2006.

[16] A. R. Djordjevic, M. B. Bazdar, T. K. Sarkar, R. F. Harrington: "AWAS for Windows: Analysis of Wire Antennas and Scatterers - Software and User's Manual," *Arctech House Books*, Boston, 1995.

Vesna Javor was born in Niš, Serbia, in 1961. She received B. Sc. and M. Sc. degrees from the Faculty of Electronic Engineering of Niš, in 1985 and 1999. From 1989 to 1991 she was the system analyst and the chief of Data Processing Department in Zadar, Croatia. She is currently teaching assistant at the Faculty of Electronic Engineering of Niš. She is the author or co-author of about fourty papers at international and national conferences, in journals and of several textbooks. Her main research interests are antennas, lightning protection, electromagnetic compatibility, electrical circuit theory and computer programs for electromagnetics.